







ORIGINAL RESEARCH

Cytokine Adsorption During Ex Vivo Blood Perfusion Improves Contractility of Donation After Circulatory Death Hearts

Lars Saemann , PhD; Sabine Pohl, TA; Kristin Wächter , PhD; Adrian-Iustin Georgevici , MD; Conny Köhler, PhD; Jennifer Jünger, PhD; Fabio Hoorn, BSc; Nitin Gharpure; Anne Großkopf , PhD; Sevil Korkmaz-Icöz , PhD; Folker Wenzel, MD, PhD; Matthias Karck, MD, PhD; Andreas Simm , PhD; Gábor Szabó, MD, PhD

BACKGROUND: Donation after circulatory death (DCD) hearts have to withstand ischemia/reperfusion injury that is partially driven by proinflammatory cytokines and decreases ventricular contractility. We hypothesize that cytokine adsorption during normothermic ex vivo blood perfusion of DCD hearts reduces the cytokine levels and improves ventricular contractility.

METHODS AND RESULTS: Porcine DCD hearts were maintained 4 hours by ex vivo blood perfusion with (DCD-BP^{CytoS}, all groups: N=8) or without (DCD-BP) CytoSorb, followed by 2 hours reperfusion with fresh blood, including left ventricular functional analysis using a balloon catheter. In a control and a DCD group, hearts were evaluated after procurement. We determined lactate and cytokines after ex vivo blood perfusion and the myocardial and left anterior descending artery transcriptome using microarrays after reperfusion. In DCD-BP^{CytoS}, the developed pressure (control: 124±7 mm Hg/s, DCD: 86±4 mmHg/s, DCD-BP: 69±11 mmHg/s, DCD-BP^{CytoS}: 112±9 mmHg/s; $P<0.05$) and maximal slope of pressure increment (control: 2010±39 mmHg/s, DCD: 1219±164 mmHg/s, DCD-BP: 964±163 mmHg/s, DCD-BP^{CytoS}: 1794±205 mmHg/s; $P<0.05$) were higher compared with DCD-BP and DCD hearts. However, contractility decreased later during reperfusion without CytoSorb. After 4 hours, troponin, lactate (45±5% versus 69±9%, $P<0.05$), IL (interleukin)-1 β , -1ra, and -8 were lower in DCD-BP^{CytoS} hearts. In the myocardium of DCD-BP^{CytoS} compared with DCD-BP hearts, inflammatory mediator receptor activity/binding pathways were enriched, and pathways for collagen-containing extracellular matrix and contractile fiber were underrepresented. In the left anterior descending artery of DCD-BP^{CytoS} hearts, serine/threonine/tyrosine kinase activity and wound-healing pathways were enriched, and mitochondrial protein-containing complex and respiratome-associated pathways were underrepresented.

CONCLUSIONS: CytoSorb during ex vivo blood perfusion enhances the maintenance of DCD hearts and is likely to improve graft function after transplantation.

Key Words: cytokine adsorption ■ cytokines ■ CytoSorb ■ donation after circulatory death ■ heart transplantation ■ machine perfusion

Donation from circulatory death (DCD) has increased the number of heart transplantations (HTXs).^{1–3} DCD hearts are exposed to warm ischemia in the donor, followed by a flush with a cold preservation solution and subsequent reperfusion with warm blood in the ex vivo blood perfusion (EVBP) device for

transportation.¹ Ischemia/reperfusion injury (IRI), the consequence of consecutive periods of ischemia and reperfusion, decreases ventricular contractility after transplantation and causes primary graft dysfunction, which if severe can increase mortality after HTX. Thus, different approaches have been investigated to reduce

Correspondence to: Lars Saemann, University Hospital Halle, Ernst-Grube-Straße 40, 06120 Halle (Saale), Germany. Email: lars.saemann@uk-halle.de

This article was sent to June-Wha Rhee, MD, Associate Editor, for review by expert referees, editorial decision, and final disposition.

Supplemental Material is available at <https://www.ahajournals.org/doi/suppl/10.1161/JAHA.124.036872>

For Sources of Funding and Disclosures, see page 15.

© 2024 The Author(s). Published on behalf of the American Heart Association, Inc., by Wiley. This is an open access article under the terms of the [Creative Commons Attribution-NonCommercial-NoDerivs](https://creativecommons.org/licenses/by-nc-nd/4.0/) License, which permits use and distribution in any medium, provided the original work is properly cited, the use is non-commercial and no modifications or adaptations are made.

JAHA is available at: www.ahajournals.org/journal/jaha

RESEARCH PERSPECTIVE

What New Question Does This Study Raise?

- Cytokine adsorption during ex vivo blood perfusion of hearts donated after circulatory death improves graft maintenance in a porcine model.

What Question Should Be Addressed Next?

- Future studies should investigate whether cytokine adsorption should be continued in the donor immediately after orthotopic heart transplantation.

Nonstandard Abbreviations and Acronyms

DCD	donation from circulatory death
DP	developed pressure
ECM	extracellular matrix
EVBP	ex vivo blood perfusion
GE	gene expression
hs-TnT	high-sensitivity troponin T
HTX	heart transplantation
IRI	ischemia/reperfusion injury
PARP	poly(adenosine diphosphate-ribose) polymerase

the IRI in DCD hearts, mainly in a preclinical setting. Hypothermic, oxygenated machine perfusion with a crystalloid preservation solution with multiple protective substances effectively reduced myocardial IRI in porcine DCD hearts.⁴ Another group investigated hypothermic, oxygenated machine perfusion with a crystalloid preservation solution with added packed red cells⁵ or whole blood.⁶ We also investigated the effect of pharmacological supplementation during EVBP on myocardial microcirculation of DCD hearts.⁷

IRI is partially driven by proinflammatory cytokines.⁸ Additionally, rewarming after hypothermia, such as during cardiac surgery with cardiopulmonary bypass or therapeutic hypothermia after resuscitation, increases cytokine production.^{9,10} After EVBP, the heart is subjected to a cold, cardioplegic arrest before transplantation into the recipient. This creates repetitive periods of normothermic and hypothermic temperatures and therefore repetitive rewarming that might induce a release of cytokines.

Furthermore, the level of proinflammatory cytokines in the blood of DCD donors is elevated. This blood is used to fill the perfusion system and recirculates continuously

through the donor heart during transportation.¹¹ Lastly, foreign body surfaces, such as the perfusion system, also trigger the release of cytokines.¹² Increased concentrations of proinflammatory cytokines and a profound IRI will likely damage the cardiac allograft and decrease DCD heart function. Cytokine adsorption is effective in reducing cytokine concentrations.¹³ Thus, we hypothesize that cytokine adsorption during EVBP improves the contractility of DCD hearts.

METHODS

The data that support the findings of this study are available from the corresponding author upon reasonable request.

Animals and Anesthesia

The investigations were reviewed and approved (35-9185.81/G-150/19). The animals received humane care. We sedated healthy pigs (40–50 kg body weight) with an intramuscular injection of ketamine (22.5 mg/kg; Bremer Pharma, Warburg, Germany) and midazolam (0.375 mg/kg; Hamelin Pharma Plus, Hamelin, Germany) and maintained the anesthesia with pentobarbital-sodium intravenously (15 mg/kg per hour; Boehringer Ingelheim Vetmedica, Ingelheim, Germany). For analgesia we administered dipidolor (1.125 mg/kg per hour; Piramal Critical Care, Voorschoten, the Netherlands). We monitored the blood pressure.

Circulatory Death Model and Study Groups

We applied a clinically relevant large animal DCD model with clinically relevant transportation and reperfusion periods for the donor heart. We performed a median sternotomy, exposed the heart, and injected heparin (LEO Pharma, Neuisenburg, Germany) intravenously. According to the previously published model, we induced global ischemia followed by circulatory death by the termination of mechanical ventilation.¹⁴ Within the subsequent period of 30 minutes, after the termination of mechanical ventilation, we also collected blood to prime the perfusion system. At the end of the 30 minutes, the hearts were flushed with 2 L of cold (4 °C) Custodiol (Köhler Chemie GmbH, Bensheim, Germany) preservation solution and harvested (Figure 1).

After harvesting, we maintained the DCD hearts for 4 hours by normothermic blood perfusion through the ascending aorta as if they had been transported to a transplantation hospital. Depending on the group, we performed the blood perfusion with (DCD-BP^{CytoS}; N=8) or without (DCD-BP; N=8) a cytokine adsorber (CytoSorb; Cytosorbents Europe, Berlin, Germany). After transportation perfusion, we initiated a 2-hour

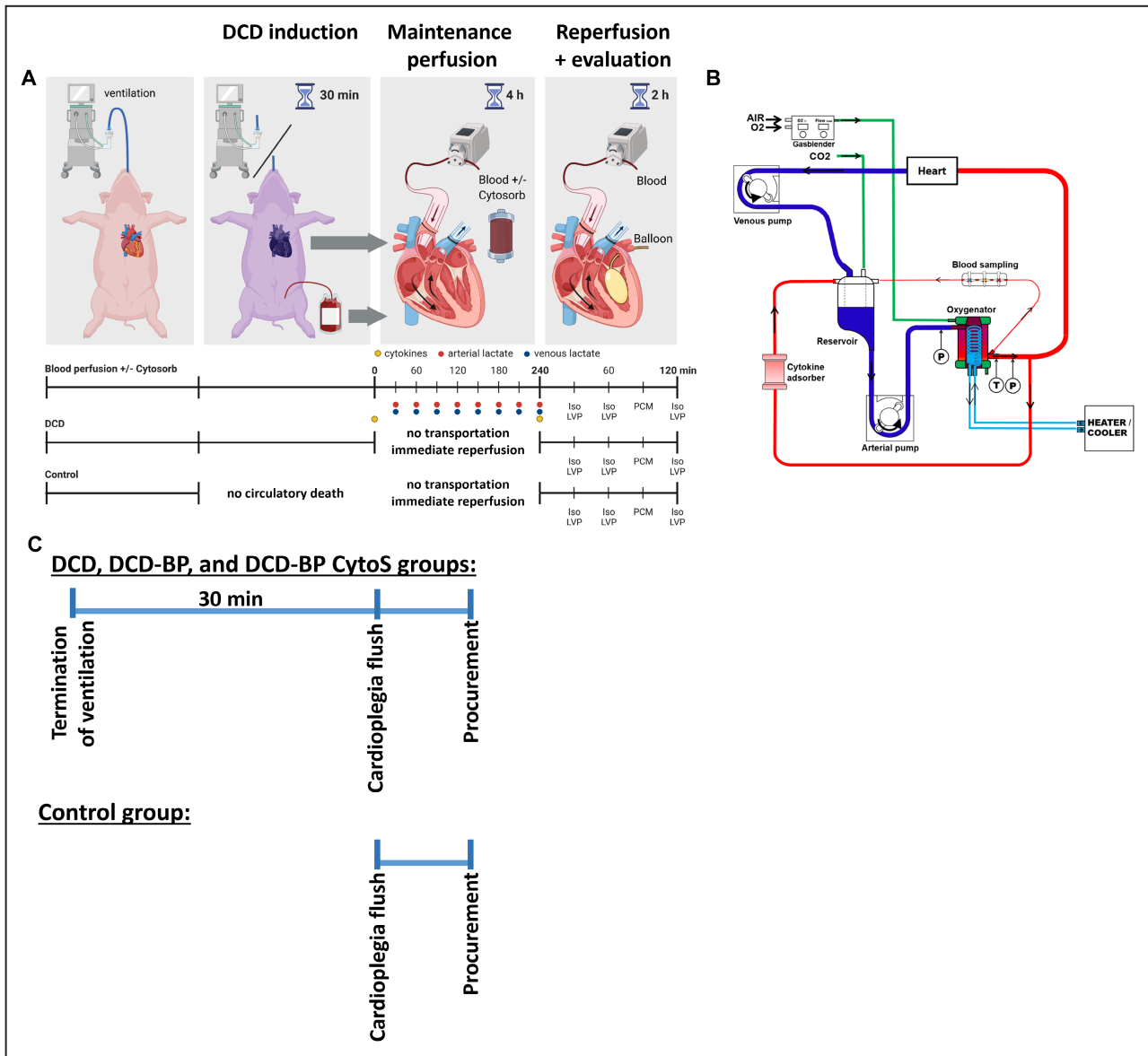


Figure 1. Workflow.

A, DCD model and blood sample collection (marked by blue, red, and yellow dots). **B**, Perfusion system. **C**, Ischemic period and procurement workflow. DCD indicates donation after circulatory death; DCD-BP, donation after circulatory death hearts blood perfusion without CytoSorb; DCD-BP CytoS, donation after circulatory death hearts blood perfusion pump with CytoSorb; LVP, left ventricular pressure; and PCM, pressure contractility matching.

transplantation-equivalent reperfusion period with fresh blood, including contractile assessment, to mimic the situation after transplantation. During this period, no adsorber was used. In another DCD group (DCD; N=8), the 2-hour reperfusion period with fresh blood, including contractile assessment, was performed immediately after harvesting, without a transportation period of 4 hours. In a control group (control; N=8), native hearts were flushed with 2L of cold (4°C) Custodiol preservation solution to induce cardioplegic arrest, harvested, and immediately reperfused and assessed for contractile function for 2 hours.

Maintenance Perfusion and Reperfusion With Blood

The perfusion system comprised an open venous reservoir and a hollow-fiber membrane oxygenator (Figure 1). Heparin (5000 IU), sodium chloride, magnesium chloride, glucose, sodium-prednisolone, sodium hydrogen carbonate, and mannitol were added. We adjusted the paO_2 to 180 to 200 mmHg, $paCO_2$ to 35 to 45 mmHg, and pH to 7.35 to 7.45. We applied a pressure-controlled perfusion with 50 to 60 mmHg. We measured arterial and venous blood gas and lactate every 30 minutes (RAPID Point 500; Siemens). We

also measured lactate every 30 minutes to perfectly mimic the clinical procedure of EVBP, where lactate, although criticized in the literature, is used as a surrogate parameter to evaluate the metabolic state of the heart.¹⁴

Functional Analysis

During functional analysis, the hearts were paced at 80 beats/min. To investigate the development of left ventricular contractility, we assessed the end-systolic pressure, end-diastolic pressure, the maximal slope of pressure increment, and minimum slope of pressure decrement at 30, 60, and 120 minutes of reperfusion at a perfusion pressure of 60 mmHg with a left ventricular balloon catheter inserted through the mitral valve. Ventricular contractility changes by ventricular filling volumes. Thus, we investigated contractility at different balloon filling volumes of 5, 10, 15, and 20 mL to provide a comprehensive contractile evaluation. Additionally, we measured pressure contractility matching at a constant left ventricular filling of 10 mL and differing perfusion pressures. The perfusion pressure was adjusted by changing the pump's revolutions per minute, thereby adjusting pump flow. We also derived the developed pressure (DP), an accurate systolic parameter, from the end-systolic pressure by subtracting the end-diastolic pressure.

Cytokine Profiling

We profiled the perfusate concentration of 13 cytokines from serum samples at the beginning and the end of the 4-hour transportation perfusion, using a porcine cytokine/chemokine magnetic bead panel (Milliplex Map Kit; EMD Millipore, Merck, Darmstadt, Germany) and a Bio-Plex 200 (Bio-Rad, Feldkirchen, Germany) according to the manufacturer's instructions. In brief, serum samples were incubated with magnetic beads at 4 °C for 14 to 18 hours, followed by incubation with detection antibodies and later streptavidin-phycoerythrin. All incubations were performed with agitation. We included all out-of-range low values as a concentration of 0 ng/mL in the analysis.

Tissue Collection

We flushed the hearts with an ice-cold Ringer solution at the end of the transplantation-equivalent reperfusion period. Myocardial tissue samples were immediately snap-frozen in liquid nitrogen. The left anterior descending (LAD) artery, including surrounding myocardial tissue, was quickly excised and placed in an ice-cold carbonized Krebs-Henseleit buffer solution. Under microscopic vision, the LAD artery was carefully but quickly dissected and snap-frozen in liquid nitrogen. All tissue samples were stored at -80 °C until

further investigation. We also conserved additional tissue samples in paraformaldehyde solution and embedded them in paraffin to be cut into 1.5- μ m-thick slices, which were placed on adhesive slides.

Cardiac Enzymes

We measured hs-TnT (high-sensitivity troponin T) with a clinical routine laboratory process to determine the myocardial injury at the end of EVBP.

Immunohistochemical Staining of Poly(Adenosine Diphosphate-Ribose) Polymerase

Immunohistochemical staining of PARP (poly(adenosine diphosphate-ribose)polymerase) (ab191217; Abcam, China), a marker of necrosis, and terminal deoxynucleotidyl transferase dUTP nick end labeling (kit 10625; Invitrogen) staining to detect apoptotic cells by labeling of DNA double-strand breaks were performed, according to the manufacturer's instructions.

RNA Preparation

Total RNA was isolated from the left ventricular myocardium and LAD artery of every pig (N=8 per group; N=32 in total). RNA was isolated by TRIzol (Thermo Fisher Scientific, Waltham, MA) extraction. Therefore, the samples were homogenized using a Tissue Lyser II (Quiagen, the Netherlands). Then, chloroform was added to induce phase separation. After centrifugation, the upper phase was agitated by incubation with isopropanol. Then, we pelletized the RNA by centrifugation at 4 °C and washed the pellet with sodium acetate. Then, the pellet was dissolved overnight at -20 °C in diethylpyrocarbonate-H₂O, followed by 2 washing steps with 80% ethanol for precipitation. Then, the RNA was stored in diethylpyrocarbonate-H₂O at -80 °C.

Microarrays

The myocardial and LAD artery transcriptome was determined using porcine arrays (Thermo Fisher Scientific). First, we assessed the RNA integrity using the Bioanalyzer (2100 Bioanalyzer; Agilent). We determined the RNA concentration using Nanodrop One (Thermo Fisher Scientific). Biotin-labeled single-stranded cDNA was synthesized from total RNA with a GeneChip WT Pico Reagent Kit (Thermo Fisher Scientific), fragmented, and subsequently hybridized using porcine arrays (Thermo Fisher Scientific). Afterward, the chips were washed and scanned by the Affymetrix GeneChip Scanner 7G. One control group sample was identified as an outlier based on principal component analysis and therefore excluded. We also performed a functional annotation analysis for the identification of enriched gene ontology-based sets.¹⁵

Quantitative Real-Time Polymerase Chain Reaction

The iScript Advanced cDNA Synthesis Kit (Bio-Rad) was used to generate cDNA from RNA, according to the manufacturer instructions. Quantitative real-time polymerase chain reaction was performed with the obtained cDNA using the SsoAdvanced Universal SYBR Green Supermix Kit (Bio-Rad) together with specific forward and reverse primers (listed in Table S1) on the CFX Connect Real-Time System (Bio-Rad). The mRNA expression levels of the target genes were normalized on expression levels of the reference gene (glyceraldehyde-3-phosphate-dehydrogenase for myocardium and hypoxanthine-guanine-phosphoribosyltransferase for LAD artery) and calculated by the $\Delta\Delta C_t$ method.

Statistical Analysis

Results are expressed as mean \pm SEM. We tested for homogeneity of variances by the Levene test using IBM SPSS Statistics for Windows (version 25.0; IBM, Armonk, NY). Functional data were analyzed using 1-way analysis of variance followed by post hoc tests according to Tukey in the case of variance homogeneity and Games-Howell in the case of variance inhomogeneity. For lactate and cytokine comparison, a 2-tailed unpaired *t* test (variance homogeneity) and a Welch *t* test (variance inhomogeneity) were applied. A value of $P < 0.05$ was considered statistically significant.

Heat maps and volcano plots were built using the Transcriptome Analysis Console version 4.0 (Applied Biosystems; Thermo Fisher Scientific). Differentially expressed genes were displayed through fold change (upregulated >2.0 ; down-regulated <-2.0), together with a *P* value <0.01 using eBayes statistics.

Next to the measured gene expression (GE) from the myocardium and LAD artery, we also computed the difference of myocardial and LAD GE (ΔGE) per animal: $\Delta GE = GE_{\text{myocardium}} - GE_{\text{LAD}}$. If a gene was significantly (<0.05) regulated across all groups in the myocardial or LAD artery expression or ΔGE according to a prefilter step using Kruskal-Wallis, it was included in the further analysis. In the second step, we performed variable selection by applying the Boruta machine-learning method for variable selection to identify the GE that is informative for group classifications. The Boruta algorithm uses ensembles of decision trees to estimate nonparametrically multivariate and nonlinear associations. As such, a variable is confirmed as informative if the variable-importance distribution is statistically significant at the Bonferroni-corrected *P* value <0.01 . A total of 1000 Boruta iterations were computationally allowed. NormHits represents the percent of iterations where the variable importance of data is higher than its permutation.¹⁶ We explored how multiple variables separate

across groups using the C.50 tree algorithm.¹⁷ We also performed a GE network analysis to identify correlating genes as described in Data S1. The edges between nodes are the absolute values of the Pearson correlation coefficients if the false discovery rate-adjusted *P* values were significant. The pathfindR package was used to identify significantly enriched pathways. Then the 10 most enriched paths in 4 categories, cellular component, biological process, molecular function, and human phenotype ontology, were plotted for specific group and tissue comparisons. All pathways plotted are $P < 0.05$.

RESULTS

Contractile Function

The DCD group showed significantly reduced DP and maximal slope of pressure increment compared with control hearts (Figure 2). During early reperfusion, DP and maximal slope of pressure increment in DCD-BP and DCD hearts were not significantly different and then decreased by reperfusion time. The contractility in DCD-BP^{CytoS} hearts was significantly higher compared with DCD or DCD-BP hearts. After 120 minutes of reperfusion, DP was also significantly decreased compared with control hearts in the DCD-BP^{CytoS} hearts. In DCD-BP^{CytoS} hearts, minimum slope of pressure decrement was improved compared with DCD-BP hearts. The end-diastolic pressure was increased in the DCD-BP^{CytoS} hearts. During pressure contractility matching, maximal slope of pressure increment and minimum slope of pressure decrement were significantly decreased compared with the control only in DCD-BP but not in DCD-BP^{CytoS} hearts.

Lactate and Troponin

During machine perfusion, the relative lactate concentration (Figure 3A) decreased in both groups. In DCD-BP hearts, lactate decreased less and remained significantly higher than in DCD-BP^{CytoS} hearts. The baseline concentration of hs-TnT in organ donors before circulatory death induction was comparable between DCD-EVBP and DCD-EVBP^{CytoS} groups (Figure 3B). At the end of 240 minutes of maintenance perfusion, the perfusate concentration of hs-TnT was significantly lower in the DCD-EVBP^{CytoS} group (Figure 3C). In Data S1, the troponin kinetics during EVBP are shown (Data S1: Figure S1).

Cytokine Concentrations

After 240 minutes of EVBP, the concentration of IL (interleukin)-8 was significantly lower in DCD-BP^{CytoS} hearts (Figure 4) compared with DCD-BP hearts (54.8 ± 15.3 versus 4.6 ± 1.3 ng/mL; $P = 0.007$). IL-1 β and IL-1ra were also lower, even if not significantly, in

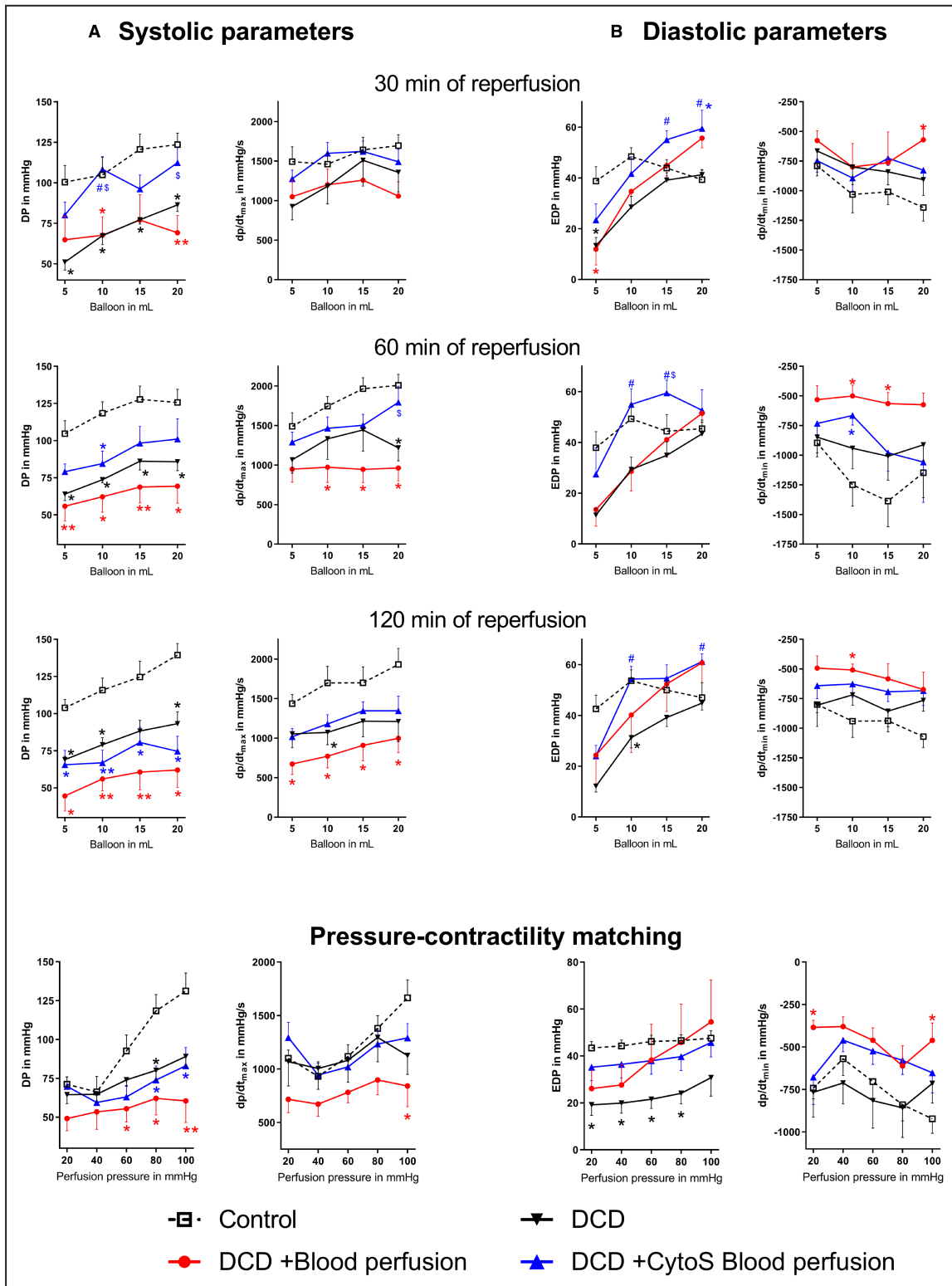


Figure 2. Left ventricular contractility. **A**, Systolic parameters. **B**, Diastolic parameters. * $P < 0.05$ vs control. ** $P < 0.001$ vs control. # $P < 0.05$ vs DCD. § $P < 0.05$ vs DCD+blood perfusion. N=8 per group. CytoS indicates CytoSorb; DCD, donation after circulatory death; DP, developed pressure; Dp/dt_{max} , slope of systolic pressure increment; Dp/dt_{min} , slope of diastolic pressure decrement; and EDP, end-diastolic pressure.

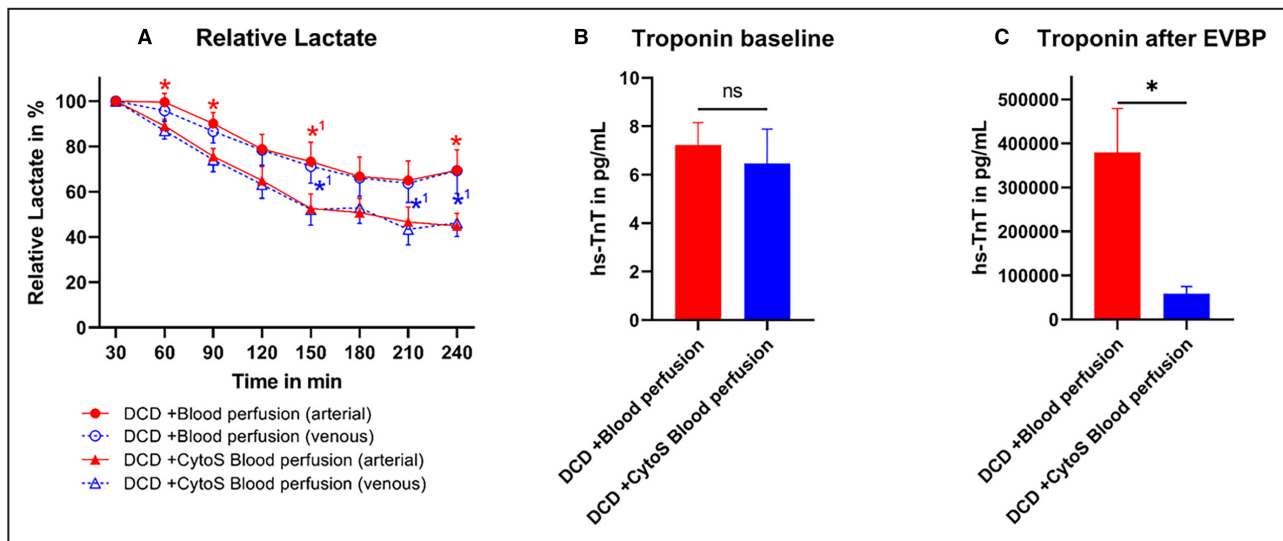


Figure 3. Metabolic markers and cardiac enzymes during maintenance perfusion.

A, Lactate during maintenance perfusion. Lactate was analyzed in relation to a baseline measurement after 30 minutes of machine perfusion. At 210 minutes of perfusion, 1 lactate sample in the DCD-BP^{CytoS} group was missing. **B**, Baseline troponin concentration in the organ donor before DCD induction. **C**, Troponin concentration in the perfusate at the end of maintenance perfusion (after 240 minutes). * $P < 0.05$ DCD-blood perfusion vs DCD-CytoS blood perfusion. * $P < 0.1$ DCD-blood perfusion vs DCD-CytoS blood perfusion. $N = 8$ per group. The error bars represent the standard error. CytoS indicates CytoSorb; DCD, donation after circulatory death; DCD-BP^{CytoS}, donation after circulatory death hearts blood perfusion with CytoSorb; EVBP, ex vivo blood perfusion; and hs-TnT, high-sensitivity troponin T.

DCD-BP^{CytoS} compared with DCD-BP hearts. The concentration of interferon (INF)- γ was higher in the DCD-BP^{CytoS} group but did not reach statistical significance. IL-6 increased in both groups during EVBP and was not significantly different. IL-1 α and IL-12 did not majorly change during EVBP in either group. Tumor necrosis factor- α , granulocyte/macrophage-colony stimulating factor, IL-2, IL-4, and IL-10 were expressed low in both groups at the beginning and end of machine perfusion.

Transcriptome and Machine-Learning Analysis

Gene expression is involved in the regulation of various processes that can impact contractility and the relaxation of the myocardium. To comprehensively investigate gene expression, we performed a microarray analysis. We found that in the myocardium, 29 genes were down- and 26 were upregulated in CytoSorb-treated hearts compared with DCD-BP hearts (Figure 5). In the LAD artery, 3 genes were down- and 53 genes were upregulated. Both groups are clearly separated from each other in the principal component analysis (Figure 5). We performed a decision tree analysis to identify the following 3 transcripts that were most characteristic for the respective group (Figure 6):

1. *Caspase 1 (CASP1)* in the LAD artery for groups with and without EVBP, independent of using

CytoSorb. It was significantly upregulated in the LAD artery of DCD-BP and DCD-BP^{CytoS} hearts compared with control hearts (Figure 6B). In the myocardium, it was also significantly upregulated in the DCD-BP^{CytoS} group compared with the DCD and DCD-BP group.

2. *Family With Sequence Similarity 104 Member A (FAM104A)* in the myocardium of DCD compared with control hearts. It was also significantly upregulated in the myocardium of both EVBP groups compared with control hearts.
3. *RAD51B* in the LAD artery for differentiation between blood perfusion with or without CytoSorb. It was significantly downregulated in the DCD-BP but not in the DCD-BP^{CytoS} compared with the DCD group.

The expression of these genes, according to the decision tree results, was confirmed by quantitative real-time polymerase chain reaction (Figure 6). To elucidate the interaction of these transcripts, we performed network analyses. The control group showed a wide, dense network, reflecting many correlations (Data S1; Figure S2). In the DCD group, the dense area of the network is shrunken. In the DCD-BP group, no defined dense area is visible anymore, and the correlations of the 3 genes identified by the decision tree with the expression of the same gene in the respective other tissue were low. We only thematize correlations of these 3 genes with transcripts of already known

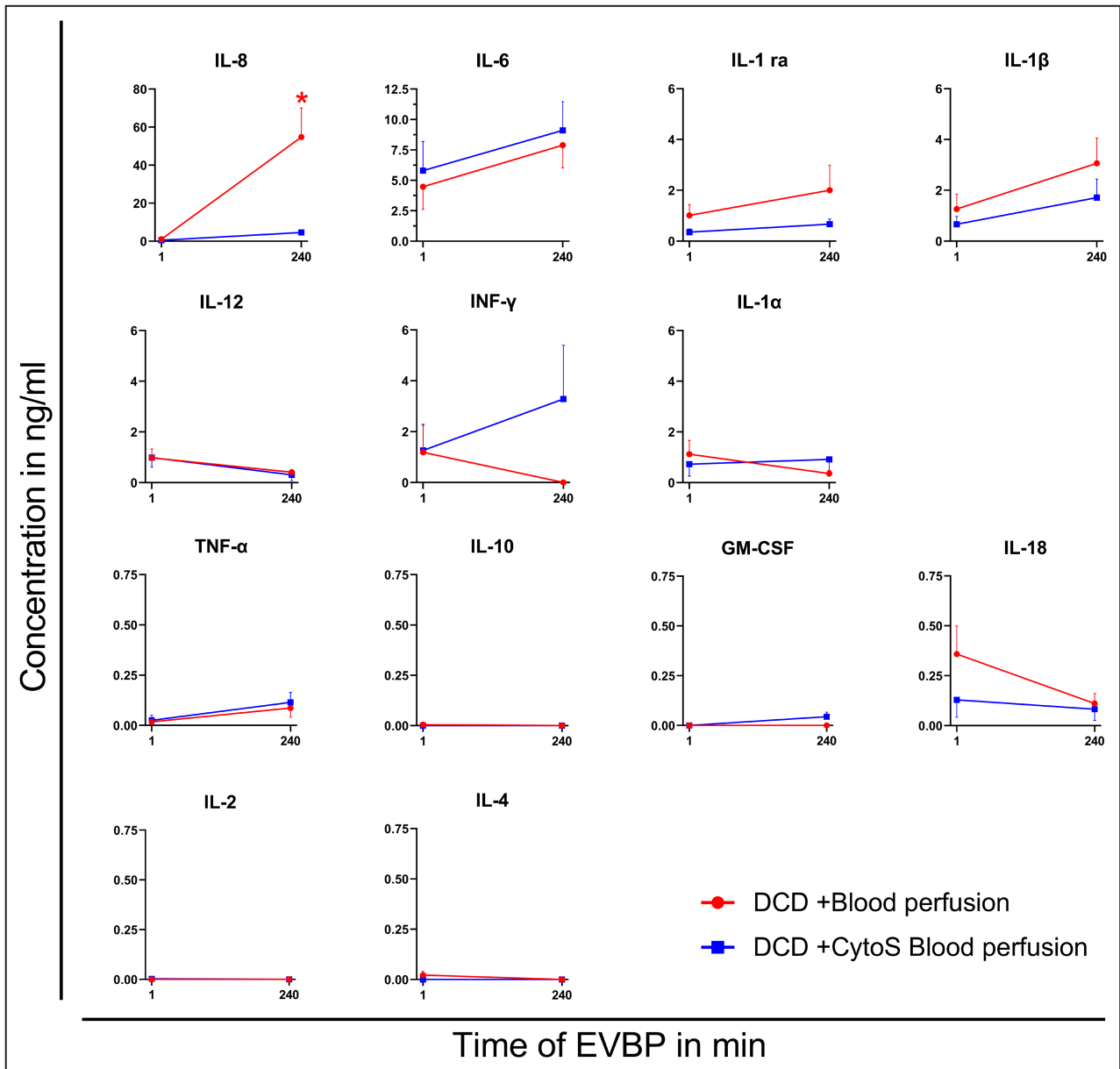


Figure 4. Cytokine concentrations during machine perfusion.

* $P < 0.05$ vs DCD+CytoS blood perfusion. N=8 per group. CytoS indicates CytoSorb; DCD, donation after circulatory death; DCD-BP, donation after circulatory death hearts blood perfusion without CytoSorb; DCD-BP^{CytoS}, donation after circulatory death hearts blood perfusion with CytoSorb; EVBP, ex vivo blood perfusion; GM-CSF, granulocyte-monocyte colony-stimulating factor; IL, interleukin; INF, interferon; and TNF, tumor necrosis factor.

functions. In DCD-BP^{CytoS} hearts, the expression of CASP1 in the LAD artery negatively correlated with the LAD expression of solute carrier family 16 member 6, chromosome 2 C5orf63 homolog, anaphase promoting complex subunit 5, and chromosome 3 open reading frame 62 C3H2orf44. In the DCD group, the myocardial expression of FAM104A correlated positively with the myocardial expression of cluster of differentiation. In the DCD-BP^{CytoS} group, we detected negative correlations with the LAD artery expression

of karyopherin subunit alpha 7. In the DCD group, RAD51B in the LAD artery correlated only with ΔGE of CASP1 positively. In the DCD-BP group, it correlated with the LAD expression of immunoglobulin superfamily member 23 and unk zinc finger. In the DCD-BP^{CytoS} group, it correlated strongly with its own ΔGE, negatively, and with ΔGE of phosphodiesterase 1A positively. It also correlated negatively with the LAD artery expression of solute carrier family 6 member 6 and positively with the LAD artery expression of proline rich

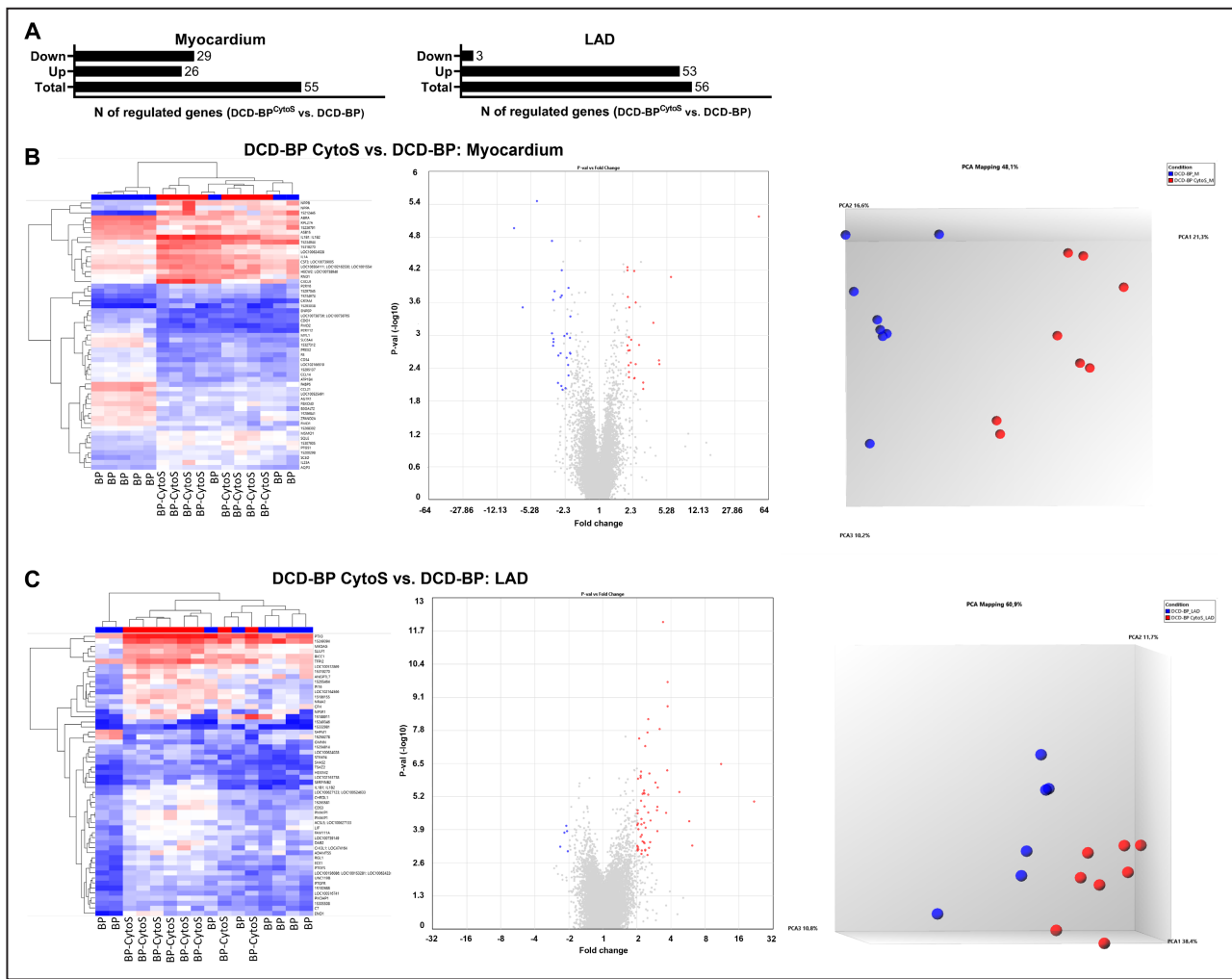


Figure 5. Regulated transcripts.

A, Myocardium and LAD artery. **B**, DCD-BP^{CytoS} vs DCD-BP; analyzed tissue: myocardium. **C**, DCD-BP^{CytoS} vs DCD-BP; analyzed tissue: LAD artery. BP indicates blood perfusion; CytoS, CytoSorb; DCD, donation after circulatory death; DCD-BP, donation after circulatory death hearts blood perfusion without CytoSorb; DCD-BP^{CytoS}, donation after circulatory death hearts blood perfusion with CytoSorb; LAD, left anterior descending; and PCA, principal component analysis.

transmembrane protein 3 and the myocardial expression of trans-activation responsive RNA-binding protein 2. The top 10 down- and top 10 upregulated genes of the DCD-BP^{CytoS} versus DCD-BP group are shown in Table 1 for the myocardium and Table 2 for the LAD artery. The functional annotation analyses of enriched gene ontology-based sets of the top 10 downregulated genes of the myocardium revealed organonitrogen compound and glycoprotein biosynthetic processes as well as response to acid chemicals as affected. Within the top 10 upregulated genes, ion and chemical homeostasis as well as positive regulation of transport were affected. The functional annotation analyses of enriched gene ontology-based sets of the top 10 upregulated genes of the LAD artery revealed fat cell differentiation as well as negative regulation of cellular process and hydrolase activity to be affected.

Pathway Analysis

The pathway analysis (Figure 7) revealed for the myocardium of DCD-BP^{CytoS} compared with DCD-BP hearts that pathways for cytokine, chemokine, and immune receptor activity or binding were enriched. Moreover, pathways for lymphocyte activation, cytokine-mediated signaling, and especially *INF-γ* production and its positive regulation were enriched. In regard to cellular components, collagen-containing extracellular matrix (ECM), contractile fiber, and oxidoreductase complex were underrepresented. For the LAD artery, comparing DCD-BP^{CytoS} to DCD-BP hearts revealed that protein kinase, serine threonine/tyrosine kinase activity, and cadherin and integrin binding were enriched. Additionally, cytokine production, wound healing, and blood vessel morphogenesis were enriched. In regard to

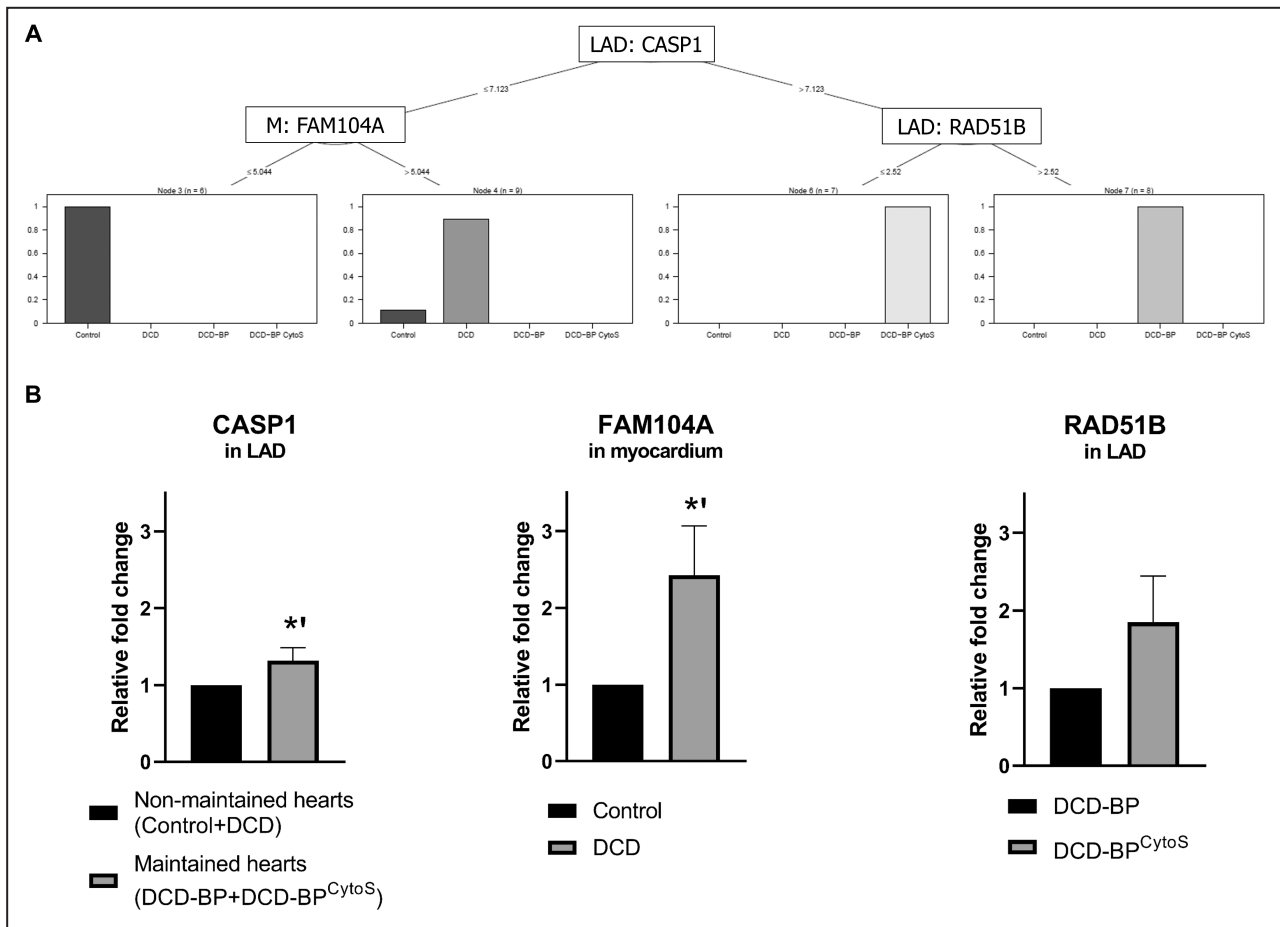


Figure 6. Identified genes.

A, Decision tree analysis. **B**, Regulation of identified genes based on RT-qPCR. * $P < 0.01$. The error bars represent the standard error. BP indicates blood perfusion; CASP1, caspase 1; CytoS, CytoSorb; DCD, donation after circulatory death; DCD-BP, donation after circulatory death hearts blood perfusion without CytoSorb; DCD-BP^{CytoS}, donation after circulatory death hearts blood perfusion with CytoSorb; FAM104A, Family With Sequence Similarity 104 Member A; LAD, left anterior descending; M, myocardium; and RT-qPCR, quantitative real-time polymerase chain reaction.

cellular components and collagen-containing ECM, external encapsulating structures were enriched, and mitochondrial protein-containing complex, ribosomal subunit, and respiratome-associated pathways were underrepresented. In the LAD arteries of both (Data S1: Figure S3) DCD-BP and DCD-BP^{CytoS} hearts compared with the myocardium, downregulated pathways were mainly mitochondrion- and oxidoreductase-associated.

Cell Death

The immunohistochemical staining of terminal deoxynucleotidyl transferase dUTP nick end labeling and PARP revealed that apoptosis of cardiomyocytes was equal between all groups, and that necrosis was the highest in the DCD group without transportation perfusion (Figure 8). In the DCD-BP and DCD-BP^{CytoS} groups, necrosis was comparable.

DISCUSSION

During the first 2 hours of reperfusion after HTX, the consequences of reperfusion injury commonly occur. Nevertheless, at the same time, the recipient is weaned off cardiopulmonary bypass, and the heart requires sufficient contractility to maintain circulation in the body.

Using CytoSorb during EVBP improved left ventricular contractility and relaxation during early reperfusion. However, after proceeding with reperfusion the DP decreased, suggesting that CytoSorb treatment needs to be continued during the early reperfusion. This suggestion is consistent with a case series showing the effective use of CytoSorb treatment intraoperatively during HTX.¹⁸ The lower lactate concentration in DCD-BP^{CytoS} group reflects that the metabolic state of the hearts of both groups differs, and that the

Table 1. Top 10 Downregulated and Top 10 Upregulated Genes in the Myocardium of DCD-BP^{CytoS} Versus DCD-BP Hearts

Fold change	P value	FDR P value	Gene symbol	Description
Downregulated				
-8.01	1.07E-05	0.0909	FABP5	Fatty acid binding protein 5 (psoriasis-associated)
-4.56	3.46E-06	0.0839	FMO2	Flavin containing monooxygenase 2 (nonfunctional)
-3.17	0.0009	0.4496	SLC6A4	Solute carrier family 6 (neurotransmitter transporter), member 4
-3.09	0.0002	0.2274	CCL21	Chemokine (C-C motif) ligand 21
-3.07	0.0015	0.5059	ZFAND2A	Zinc finger, AN1-type domain 2A
-3.05	0.0011	0.4944	ABRA	Actin binding Rho activating protein
-3.04	0.0013	0.5015	FBXO40	F-box protein 40
-2.96	0.0002	0.2099	LOC100525491	Rho GTPase-activating protein 7
-2.73	0.0073	0.9508	RPL27A	Ribosomal protein L27a
-2.56	0.0021	0.5911	B3GALT2	UDP-Gal:βGlcNAc β1,3-galactosyltransferase, polypeptide 2
Upregulated				
2.13	0.0018	0.5595	AQP3	Aquaporin 3 (Gill blood group)
2.37	6.58E-05	0.1327	P2RY6	Pyrimidinergic receptor P2Y, G-protein coupled, 6
2.38	0.0061	0.8797	SC5D	Sterol-C5-desaturase
2.41	0.006	0.8785	LOC106504111; LOC102162530; LOC100155494	Aldehyde dehydrogenase family 1 member A3-like; aldehyde dehydrogenase family 1 member A3
2.47	0.0002	0.234	HECW2; LOC100738946	HECT, C2 and WW domain containing E3 ubiquitin protein ligase 2; E3 ubiquitin-protein ligase HECW2-like
2.67	0.0015	0.5059	IL1A	Interleukin 1, α
3.78	0.0006	0.3442	IL1B1; IL1B2	Interleukin 1, β1; interleukin 1, β2
4.35	0.0029	0.6813	CXCL9	Chemokine (C-X-C motif) ligand 9
4.42	0.0033	0.7042	RND1	Rho family GTPase 1
5.84	8.39E-05	0.1526	NPPB	Natriuretic peptide B

Uncharacterized and pseudogenes were excluded. DCD-BP indicates donation after circulatory death hearts blood perfusion without CytoSorb; DCD-BP^{CytoS}, donation after circulatory death hearts blood perfusion with CytoSorb; and FDR, false discovery rate.

metabolic demand of the hearts was met in the DCD-BP^{CytoS} group. CytoSorb has, if any, only negligible direct effects on lactate levels, because lactate is a water-soluble anion of small molecular size.¹⁹

Induction of circulatory death based on ischemia due to the lack of oxygen in the body followed by reperfusion in the ex vivo machine perfusion system during transportation is a classical ischemia/reperfusion situation that commonly is associated with troponin release. Thus, an elevation of troponin during the transportation period was expected. Because the heart is maintained in a single organ perfusion system where released substances cannot be eliminated, troponin was also expected to accumulate over time and reach high concentrations. Additionally, the priming volume of the organ perfusion system is lower than the total blood volume in the human body, which also leads to high concentrations. Both aspects have been discussed in the literature previously.^{4,20,21} However,

we did not observe a profound troponin release in the CytoSorb-treated hearts. Because lactate also is an indirect biomarker for myocardial protection and function, the quicker lactate reduction in the CytoSorb-treated group also suggests a protective effect of the CytoSorb treatment. Considering that the troponin concentration was highly reduced in the DCD-BP^{CytoS} group, it appears likely that troponin might have reached a low concentration, not only because of a lower release but also due to binding to the adsorber to a certain extent. However, in the present setup, it cannot be quantified exactly to which extent it has been bound.

Cytokines

The decreased concentrations of IL-8, IL-1β, and IL-1ra in DCD-BP^{CytoS} hearts can partially explain the superior contractility and microvascular function. IL-8 is a

Table 2. Top 10 Downregulated and Top 10 Upregulated Genes in the Left Anterior Descending Artery of DCD-BP^{CytoS} Versus DCD-BP Hearts

Fold change	P value	FDR P value	Gene symbol	Description
Downregulated				
-2.19	0.0024	0.4873	SHFM1	Split hand/foot malformation (ectrodactyly) type 1
-2.07	0.0022	0.4619	GMNN	Geminin, DNA replication inhibitor
Upregulated				
3.02	0.0006	0.2681	PTX3	Pentraxin 3, long
3.03	0.0005	0.2589	CHRDL1	Chordin-like 1
3.03	0.0021	0.4619	LOC100624028	cis-aconitate decarboxylase-like
3.06	0.0001	0.1325	SERPINB2	Serpin peptidase inhibitor, clade B (ovalbumin), member 2
3.18	3.60E-06	0.0183	LOC100627123; LOC100524633	Platelet-derived growth factor receptor α
3.62	0.0007	0.2899	LOC102164566	Uncharacterized LOC102164566
3.72	4.83E-05	0.0879	NR4A2	Nuclear receptor subfamily 4, group A, member 2
3.72	1.92E-07	0.0024	MEDAG	Mesenteric estrogen-dependent adipogenesis
4.76	0.0002	0.1553	IL1B1; IL1B2	Interleukin 1, β 1; interleukin 1, β 2
5.8	0.0012	0.3711	NPSR1	Neuropeptide S receptor 1

Uncharacterized and pseudogenes were excluded. DCD-BP indicates donation after circulatory death hearts blood perfusion without CytoSorb; DCD-BP^{CytoS}, donation after circulatory death hearts blood perfusion with CytoSorb; and FDR, false discovery rate.

neutrophil chemoattractant/activator and is commonly increased after prolonged cardiac ischemia, such as after cold static storage during HTX.²² Furthermore, it is an important mediator for reperfusion injury and correlates with decreased left ventricular function in the acute phase after myocardial infarction.²³ Inhibition of IL-8 by neutralizing antibodies reduces myocardial ischemia/reperfusion injury and improves ventricular contractility.²⁴ An in vitro study by Joulin et al suggests that IL-8 is at least involved in directly reducing cardiomyocyte contractility.²⁵ Also, IL-1 β directly leads to cardiomyocyte depression, as shown by another in vitro series. IL-1 β inhibits the voltage-dependent calcium (Ca²⁺) current in cardiomyocytes, reduces β adrenergic response,²³ and finally induces cardiomyocyte systolic dysfunction.^{26,27} It also induces apoptosis.²⁷ The increased concentration of IL-1 β after nonejecting EVBP of hearts and the associated decline of systolic function is also in line with a publication by Hatami et al.²⁸ IL-1ra is anti-inflammatory,²³ inhibits the effects of IL-1 α and β , and might have been released more in DCD-BP hearts as a counter-regulation to the higher levels of IL- β ,²⁷ or it was adsorbed in DCD-BP^{CytoS} hearts.

Gene Expression

CASP1, which was significantly upregulated in both EVBP groups, cleaves and thus activates the proinflammatory cytokines IL-1 β and IL-18 and thereby initiates an inflammatory response.^{29,30} It also initiates pyroptosis.³¹ Based on this finding, cytokine adsorption during

EVBP is reasonable. Accordingly, the concentration of IL-18 was lower in DCD-BP^{CytoS} hearts (Figure 4). RAD51B is involved in the homologous recombination repair of double-stranded DNA breaks, whereas overexpression causes cell cycle G1 delay and apoptosis.³² Thus, the expression of RAD51B in the LAD artery in DCD-BP^{CytoS} hearts, which was comparable to control hearts, suggests less tissue damage. Compared with DCD and control hearts, the downregulation in DCD-BP hearts might be reactive due to a presumed upregulation beforehand. The role of FAM104A in this context still needs to be identified. Importantly, we point out that the biostatistical procedure of the decision trees does not require statistical group differences. Thus, the quantitative real-time polymerase chain reaction results do not necessarily need to reproduce statistical group differences.

Top 10 Up- and Downregulated Genes

Fatty acid binding protein 5 (FABP5) is important for cardiac mitochondrial function and was reduced in the DCD-BP^{CytoS} group.³³ FABP5 is required to transport fatty acids into the cardiomyocytes to meet the metabolic demands of the heart.³⁴ Consequently, the metabolic needs might have been lower or were already met in hearts treated with CytoSorb, and thus FABP5 might also have been downregulated. Solute carrier family 6 member 4 deficiency contributed to the development of myocardial fibrosis³⁵ and was downregulated in the DCD-BP^{CytoS} group. Increased circulating C-C motif chemokine ligand 21, expressed

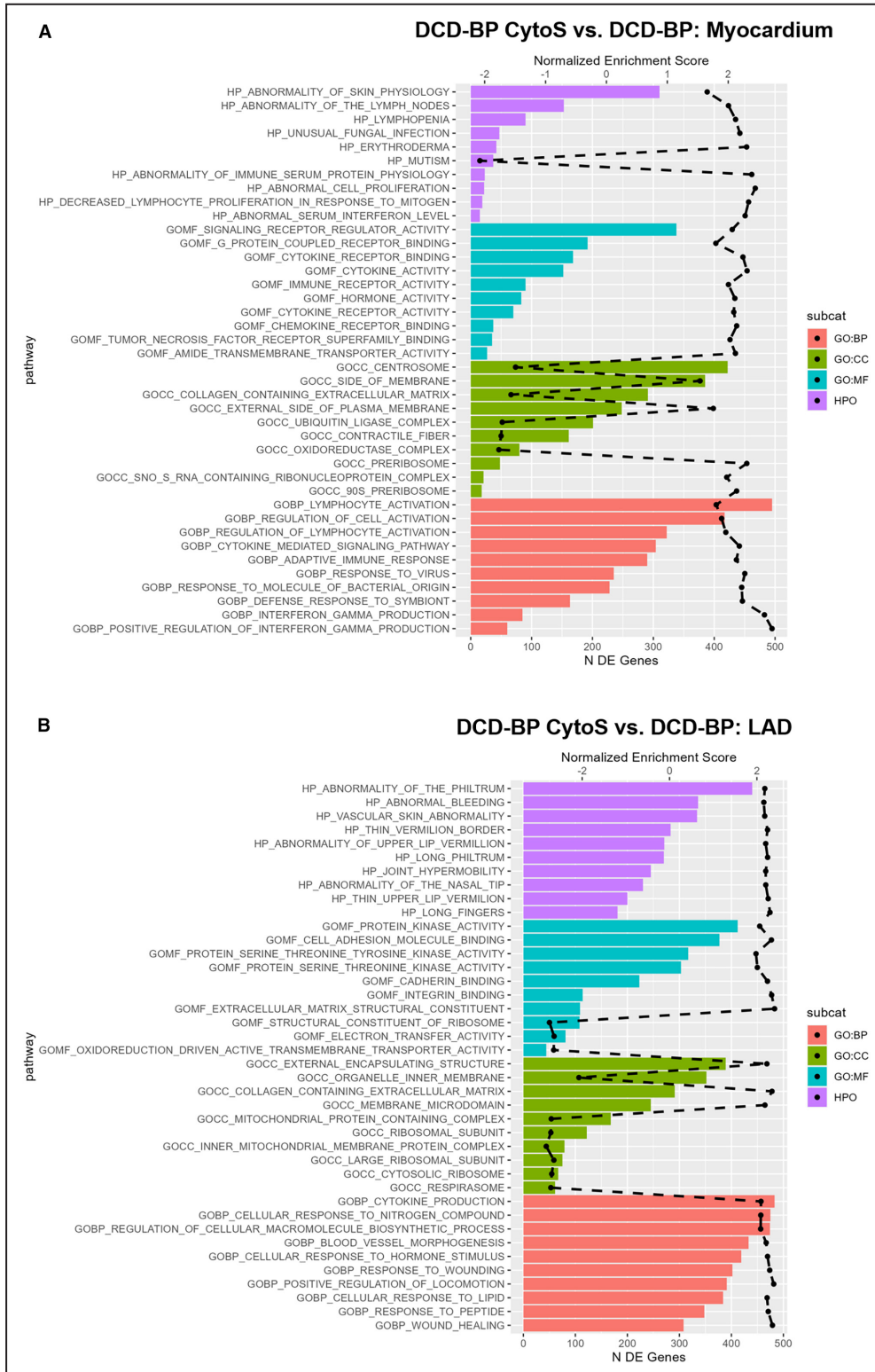


Figure 7. Pathway analysis for treatment comparison.

The dashed black line represents the normalized enrichment score. All plotted pathways are $P < 0.05$. BP indicates biological process; CC, cellular component; DCD-BP, donation after circulatory death hearts blood perfusion without CytoSorb; DCD-BP CytoS, donation after circulatory death hearts blood perfusion with CytoSorb; DE, differentially expressed; GO, gene ontology; HPO, human phenotype ontology; and MF, molecular function.

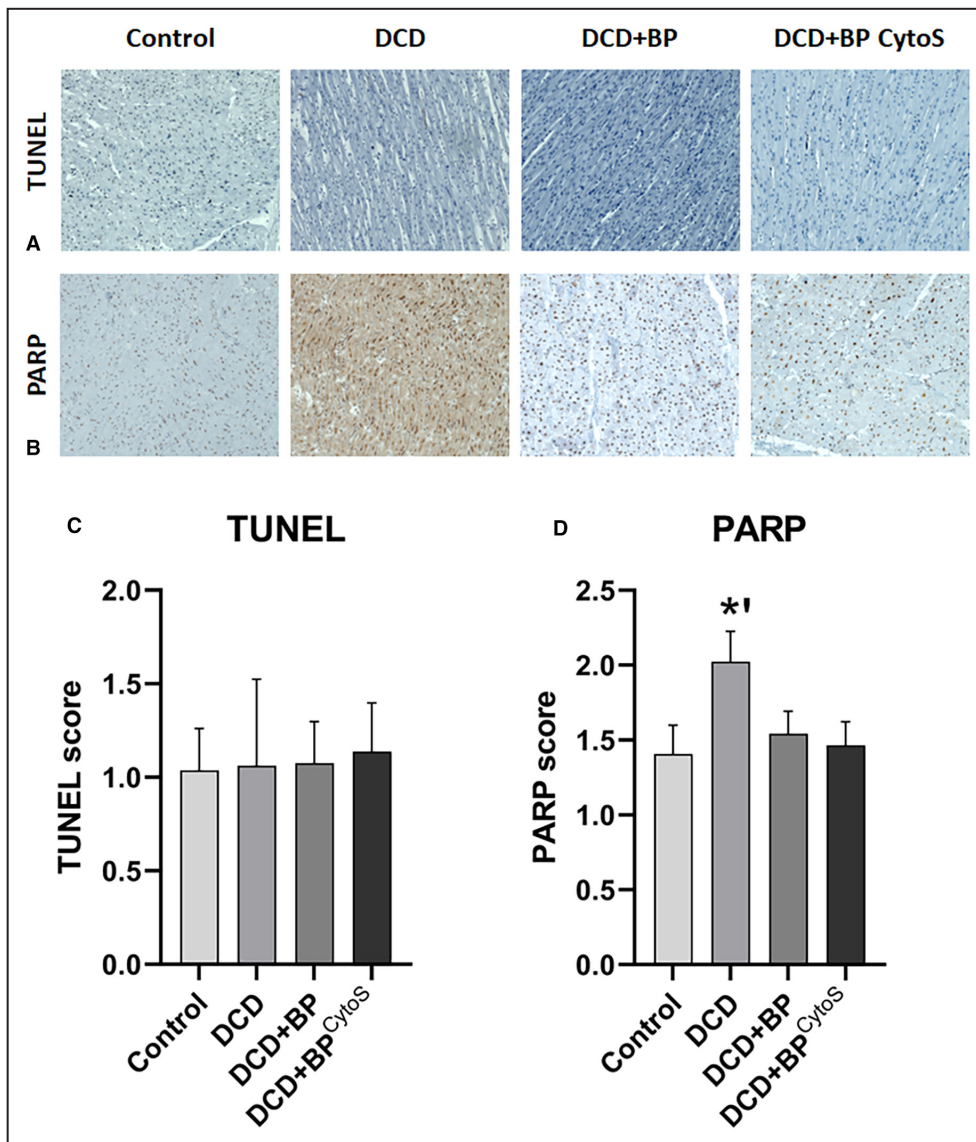


Figure 8. Immunohistochemical staining of PARP and TUNEL. The error bars represent the standard error. * $P < 0.01$. DCD indicates donation after circulatory death; DCD-BP, donation after circulatory death hearts blood perfusion without CytoSorb; DCD-BP^{CytoS}, donation after circulatory death hearts blood perfusion with CytoSorb; PARP, poly(adenosine diphosphate-ribose) polymerase; and TUNEL, terminal deoxynucleotidyl transferase dUTP nick end labeling.

higher in the non-CytoSorb-treated hearts, is associated with increased cardiovascular mortality in patients with heart failure,³⁶ and consequently fits together with the decreased contractility in the DCD-BP group. Actin-binding Rho-activating protein (*ABRA*) promotes angiogenesis.³⁷ Thus, the downregulation of *ABRA* in CytoSorb-treated hearts might reflect that the myocardium in these hearts was well perfused. The role of other genes, such as F-Box protein 40, needs further investigation.³⁸ Transcripts of *IL-1*, *IL-1β*, and *IL-1β2* might have been upregulated in the DCD-BP^{CytoS} group in reaction to the adsorption of these cytokines, which is visible in Figure 4. Pyrimidinerbic receptor P2Y6, which

was upregulated in the DCD-BP group, contributes to the development of arteriolar myogenic tone and thus vasoconstriction, and might contribute to impaired tissue perfusion.³⁹ Low tissue perfusion leads to functional decline and higher lactate release.

Nuclear receptor subfamily 4 group A member 2 was upregulated in the LAD artery of the DCD-BP^{CytoS} group and might be protective against post-myocardial infarction injury⁴⁰ (Table 2). Chordin-like 1 is protective against myocardial infarction and leads to less cardiomyocyte death and fibrosis and was upregulated in the DCD-BP^{CytoS} group. Equivalent to the myocardium, *IL-1β1* and *IL-1β2* might have been upregulated in the coronary

artery because the cytokines were adsorbed and thus reduced in the CytoSorb-treated groups. The functional annotation analyses of enriched gene ontology-based sets in the myocardium and LAD artery revealed that cellular biological processes are well preserved on the gene level in the CytoSorb-treated hearts.

Pathways

Pathways for enriched INF- γ production can explain the increased INF- γ level in DCD-BP^{CytoS} hearts. This finding appears surprising on the one hand, considering the superior contractile function in DCD-BP^{CytoS} hearts after the first hour of reperfusion (Figure 2). However, the tissue samples for transcriptomic profiling were collected at the end of reperfusion, when the contractile superiority was less prominent and not significant compared with DCD-BP hearts. On the other hand, the enriched pathways associated with inflammatory mediators can explain the decreasing contractility of hearts treated with CytoSorb during EVBP by reperfusion time. Additionally, it highlights that cytokine-mediated cardiac injury and functional decline do not occur only during the biological process but seem to have a second phase, which might occur after transplantation when CytoSorb treatment is not continued. The underrepresented number of regulated genes for contractile fiber and collagen-containing ECM in DCD-BP^{CytoS} hearts suggests that the myocardium was less injured. Thus, fewer new contractile fibers need to be produced, and presumably provisional ECM needs to be built to form a collagen-based scar.⁴¹ The latter is a typical process after the initial infarct healing phase consisting of ECM degradation, cytokine release, and initiation of inflammatory cascades, including inflammatory cell attraction.⁴¹ The oxidoreductase complex in mitochondria is involved in reactive oxygen species formation, thus contributing to functional decline after myocardial infarction, suggesting oxidative stress in DCD-BP^{CytoS} hearts.⁴² A group of molecular functions in the LAD artery of DCD-BP^{CytoS} hearts, including the serin threonine kinase activity,⁴³ contribute to tissue repair and wound healing. Thus, the regulation of *RAD51B* was also specific to the DCD-BP^{CytoS} group. The role of cadherins and integrins in the coronary artery following IRI is not fully understood. However, both play a role in the myocardium after infarction.^{44,45} The underlying reason for the consistent underrepresentation of the designated pathways in the LAD artery compared with the myocardium is most likely caused by the higher metabolically activity of the myocardium, which is richer in mitochondria and thus exhibits aerobic respiration and electron transfer and transport.⁴⁶

Limitations

We did not perform an orthotopic transplantation for the final reperfusion. However, we reperfused the heart with

fresh blood as if it had been transplanted, which makes the reperfusion period clinically relevant. Moreover, an advantage of the reperfusion and functional assessment in Langendorff mode is that no inotropic and vasoconstrictive medication is required, which would likely be needed in an in vivo transplant model. Furthermore, this model allowed us to investigate myocardial function independent of loading conditions significantly altered after cardiopulmonary bypass in general.

CONCLUSIONS

CytoSorb treatment of porcine DCD hearts during EVBP improves left ventricular contractility and relaxation. However, to preserve this effect, the treatment might need to be continued during reperfusion after HTX, conceivably not only after removal of the aortic cross-clamp and after weaning from cardiopulmonary bypass. By using CytoSorb, some inflammatory cytokines can be reduced during EVBP. Furthermore, other substances are also likely to be reduced. A main limitation of EVBP with normothermic conditions is that multiple substances and metabolites that are released by the heart accumulated during transportation might reach toxic concentrations and could potentially harm the heart and reduce myocardial protection. Optimization of EVBP by adding an adsorber may help overcome this difficulty beyond just reducing cytokine concentrations.

CytoSorb treatment affects the transcriptome of the myocardium and LAD artery differently. *FAM104*, *CASP1*, and *RAD51B* are characteristic for the effects of circulatory death induction on the myocardium, EVBP on the LAD artery, and CytoSorb treatment on the LAD artery, respectively. The distinct impact of these genes in DCD HTX should be further elucidated. CytoSorb during EVBP of DCD hearts also affects pathways differently in the myocardium compared with the LAD artery. Furthermore, enriched pathways suggest less myocardial injury but also increased wound healing mechanisms in DCD-BP^{CytoS} hearts. Necrosis and apoptosis were comparable between CytoSorb-treated and nontreated hearts. Thus, cell death in the myocardium does not seem to have contributed to the functional differences. Further work should also focus on what other potentially toxic substances are removed by the adsorber.

ARTICLE INFORMATION

Received May 30, 2024; accepted September 30, 2024.

Affiliations

Department of Cardiac Surgery, University Hospital Halle (Saale), University of Halle, Halle, Germany (L.S., S.P., K.W., A.-I.G., C.K., J.J., N.G., A.G., S.K., A.S., G.S.); Department of Cardiac Surgery, University Hospital

Heidelberg, Heidelberg, Germany (L.S., F.H., S.K., M.K., G.S.); Department of Anaesthesiology, St. Josef Hospital, Ruhr-University Bochum, Bochum, Germany (A.-I.G.); and Faculty Medical and Life Sciences, Furtwangen University, Villingen-Schwenningen, Germany (F.W.).

Acknowledgments

The authors kindly thank the Core Facility Microarrays of Medical Faculty, University of Halle, for the analysis of RNA samples.

Sources of Funding

This project was partially funded by CytoSorbents to perform the microarray analysis. Cytokine adsorbents were kindly provided by CytoSorbents.

Disclosures

None.

Supplemental Material

Data S1

REFERENCES

- Messer S, Cernic S, Page A, Berman M, Kaul P, Colah S, Ali J, Pavlushkov E, Baxter J, Quigley R, et al. A 5-year single-center early experience of heart transplantation from donation after circulatory-determined death donors. *J Heart Lung Transplant*. 2020;39:1463–1475. doi: [10.1016/j.healun.2020.10.001](https://doi.org/10.1016/j.healun.2020.10.001)
- Chew HC, Iyer A, Connellan M, Scheuer S, Villanueva J, Gao L, Hicks M, Harkness M, Soto C, Dinale A, et al. Outcomes of donation after circulatory death heart transplantation in Australia. *J Am Coll Cardiol*. 2019;73:1447–1459. doi: [10.1016/j.jacc.2018.12.067](https://doi.org/10.1016/j.jacc.2018.12.067)
- Miñambres E, Royo-Villanova M, Pérez-Redondo M, Coll E, Villar-García S, Canovas SJ, Francisco Nistal J, Garrido IP, Gómez-Bueno M, Cobo M, et al. Spanish experience with heart transplants from controlled donation after the circulatory determination of death using thoraco-abdominal normothermic regional perfusion and cold storage. *Am J Transplant*. 2021;21:1597–1602. doi: [10.1111/ajt.16446](https://doi.org/10.1111/ajt.16446)
- Saemann L, Korkmaz-Icöz S, Hoorn F, Veres G, Kraft P, Georgevici A-I, Brune M, Guo Y, Loganathan S, Wenzel F, et al. Reconditioning of circulatory death hearts by ex-vivo machine perfusion with a novel HTK-N preservation solution. *J Heart Lung Transplant*. 2021;40:1135–1144. doi: [10.1016/j.healun.2021.07.009](https://doi.org/10.1016/j.healun.2021.07.009)
- Moeslund N, Ertugrul IA, Hu MA, Dalsgaard FF, Ilkjaer LB, Ryhammer P, Pedersen M, Erasmus ME, Eiskjaer H. Ex-situ oxygenated hypothermic machine perfusion in donation after circulatory death heart transplantation following either direct procurement or in-situ normothermic regional perfusion. *J Heart Lung Transplant*. 2023;42:730–740. doi: [10.1016/j.healun.2023.01.014](https://doi.org/10.1016/j.healun.2023.01.014)
- Saemann L, Hoorn F, Wächter K, Pohl S, Korkmaz-Icöz S, Wenzel F, Karck M, Simm A, Szabó G. (1281) HTK-N versus Del Nido cardioplegia for hypothermic machine perfusion of donation after circulatory death hearts: comparison of left-ventricular contractility and transcriptomics. *J Heart Lung Transplant*. 2023;42:S546. doi: [10.1016/j.healun.2023.02.1491](https://doi.org/10.1016/j.healun.2023.02.1491)
- Saemann L, Hoffmeister A, Pohl S, Soyer S, Wernstedt L, Luise J, Kozar B, Simm A, Szabó G. Direct procurement and perfusion supplemented with the senomorphic agent ruxolitinib improves the microvascular coronary flow in hearts donated after circulatory death in dependence on donor sex and age. *J Heart Lung Transplant*. 2024;43:S493. doi: [10.1016/j.healun.2024.02.677](https://doi.org/10.1016/j.healun.2024.02.677)
- Sharma HS, Das DK. Role of cytokines in myocardial ischemia and reperfusion. *Mediat Inflamm*. 1997;6:175–183. doi: [10.1080/09629359791668](https://doi.org/10.1080/09629359791668)
- Aibiki M, Maekawa S, Nishiyama T, Seki K, Yokono S. Activated cytokine production in patients with accidental hypothermia. *Resuscitation*. 1999;41:263–268. doi: [10.1016/S0300-9572\(99\)00052-0](https://doi.org/10.1016/S0300-9572(99)00052-0)
- Bisschops LLA, Hoedemaekers CWE, Molines TE, van der Hoeven JG. Rewarming after hypothermia after cardiac arrest shifts the inflammatory balance. *Crit Care Med*. 2012;40:1136–1142. doi: [10.1097/CCM.0b013e3182377050](https://doi.org/10.1097/CCM.0b013e3182377050)
- Ardehali A, Esmailian F, Deng M, Soltesz E, Hsieh E, Naka Y, Mancini D, Camacho M, Zucker M, LePrince P, et al. Ex-vivo perfusion of donor hearts for human heart transplantation (PROCEED II): a prospective, open-label, multicentre, randomised non-inferiority trial. *Lancet*. 2015;385:2577–2584. doi: [10.1016/S0140-6736\(15\)60261-6](https://doi.org/10.1016/S0140-6736(15)60261-6)
- Jahns G, Haeffner-Cavaillon N, Nydegger UE, Kazatchkine MD. Complement activation and cytokine production as consequences of immunological bioincompatibility of extracorporeal circuits. *Clin Mater*. 1993;14:303–336. doi: [10.1016/0267-6605\(93\)90017-2](https://doi.org/10.1016/0267-6605(93)90017-2)
- Ghaidan H, Stenlo M, Niroomand A, Mittendorfer M, Hirdman G, Gvazava N, Edström D, Silva IAN, Broberg E, Hallgren O, et al. Reduction of primary graft dysfunction using cytokine adsorption during organ preservation and after lung transplantation. *Nat Commun*. 2022;13:4173. doi: [10.1038/s41467-022-31811-5](https://doi.org/10.1038/s41467-022-31811-5)
- Saemann L, Wenzel F, Kohl M, Korkmaz-Icöz S, Hoorn F, Loganathan S, Guo Y, Ding Q, Zhou P, Veres G, et al. Monitoring of perfusion quality and prediction of donor heart function during ex-vivo machine perfusion by myocardial microcirculation versus surrogate parameters. *J Heart Lung Transplant*. 2021;40:387–391. doi: [10.1016/j.healun.2021.02.013](https://doi.org/10.1016/j.healun.2021.02.013)
- Herwig R, Hardt C, Lienhard M, Kamburov A. Analyzing and interpreting genome data at the network level with ConsensusPathDB. *Nat Protoc*. 2016;11:1889–1907. doi: [10.1038/nprot.2016.117](https://doi.org/10.1038/nprot.2016.117)
- Kursa MB, Rudnicki WR. Feature selection with the Boruta package. *J Stat Softw*. 2010;36:1–13. doi: [10.18637/jss.v036.i11](https://doi.org/10.18637/jss.v036.i11)
- Kuhn M, Johnson K. *Applied Predictive Modeling*. New York, NY: Springer; 2013. doi: [10.1007/978-1-4614-6849-3](https://doi.org/10.1007/978-1-4614-6849-3)
- Kamat NA, Gaur A, Phadke A, Waje N, Bunage R, Meeran T, Sinha S, Chavan A, Haji J, Rathod A, et al. (351) utility of intraoperative cytokine hemoadsorption therapy during cardiac transplantation. *J Heart Lung Transplant*. 2023;42:S166–S167. doi: [10.1016/j.healun.2023.02.1655](https://doi.org/10.1016/j.healun.2023.02.1655)
- Friesecke S, Stecher S-S, Gross S, Felix SB, Nierhaus A. Extracorporeal cytokine elimination as rescue therapy in refractory septic shock: a prospective single-center study. *J Artif Organs*. 2017;20:252–259. doi: [10.1007/s10047-017-0967-4](https://doi.org/10.1007/s10047-017-0967-4)
- Bona M, Wyss RK, Arnold M, Méndez-Carmona N, Sanz MN, Günsch D, Barile L, Carrel TP, Longnus SL. Cardiac graft assessment in the era of machine perfusion: current and future biomarkers. *J Am Heart Assoc*. 2021;10:e018966. doi: [10.1161/JAHA.120.018966](https://doi.org/10.1161/JAHA.120.018966)
- Sourdon J, Dombierier M, Huber S, Gahl B, Carrel TP, Tevearai HT, Longnus SL. Cardiac transplantation with hearts from donors after circulatory declaration of death: haemodynamic and biochemical parameters at procurement predict recovery following cardioplegic storage in a rat model. *Eur J Cardiothorac Surg*. 2013;44:e87–e96. doi: [10.1093/ejcts/ezt142](https://doi.org/10.1093/ejcts/ezt142)
- Oz MC, Liao H, Naka Y, Seldomridge A, Becker DN, Michler RE, Smith CR, Rose EA, Stern DM, Pinsky DJ. Ischemia-induced interleukin-8 release after human heart transplantation. A potential role for endothelial cells. *Circulation*. 1995;92:II428–II432. doi: [10.1161/01.CIR.92.9.428](https://doi.org/10.1161/01.CIR.92.9.428)
- Liu Y, Zhang D, Yin D. Pathophysiological effects of various interleukins on primary cell types in common heart disease. *Int J Mol Sci*. 2023;24:24. doi: [10.3390/ijms24076497](https://doi.org/10.3390/ijms24076497)
- Boyle EM, Kovacich JC, Hébert CA, Cauty TG, Chi E, Morgan EN, Pohlman TH, Verrier ED. Inhibition of interleukin-8 blocks myocardial ischemia-reperfusion injury. *J Thorac Cardiovasc Surg*. 1998;116:114–121. doi: [10.1016/S0022-5223\(98\)70249-1](https://doi.org/10.1016/S0022-5223(98)70249-1)
- Joulin O, Petitot P, Labalette M, Lancel S, Nevriere R. Cytokine profile of human septic shock serum inducing cardiomyocyte contractile dysfunction. *Physiol Res*. 2007;56:291–297. doi: [10.33549/physiolres.930946](https://doi.org/10.33549/physiolres.930946)
- Frangogiannis NG. Interleukin-1 in cardiac injury, repair, and remodeling: pathophysiological and translational concepts. *Discoveries (Craiova)*. 2015;3:e41. doi: [10.15190/d.2015.33](https://doi.org/10.15190/d.2015.33)
- Suzuki K, Murtuza B, Smolenski RT, Sammut IA, Suzuki N, Kaneda Y, Yacoub MH. Overexpression of interleukin-1 receptor antagonist provides cardioprotection against ischemia-reperfusion injury associated with reduction in apoptosis. *Circulation*. 2001;104:I-308. doi: [10.1161/circ.104.suppl_1.1-308](https://doi.org/10.1161/circ.104.suppl_1.1-308)
- Hatami S, White CW, Qi X, Buchko M, Ondrus M, Kinneer A, Himmat S, Sergi C, Nagendran J, Freed DH. Immunity and stress responses are induced during ex situ heart perfusion. *Circ Heart Fail*. 2020;13:e006552. doi: [10.1161/CIRCHEARTFAILURE.119.006552](https://doi.org/10.1161/CIRCHEARTFAILURE.119.006552)
- Thornberry NA, Bull HG, Calaycay JR, Chapman KT, Howard AD, Kostura MJ, Miller DK, Molineaux SM, Weidner JR, Aunins J. A novel heterodimeric cysteine protease is required for interleukin-1 beta processing in monocytes. *Nature*. 1992;356:768–774. doi: [10.1038/356768a0](https://doi.org/10.1038/356768a0)
- Gaggero A, de Ambrosis A, Mezzanzanica D, Piazza T, Rubartelli A, Figini M, Canevari S, Ferrini S. A novel isoform of pro-interleukin-18 expressed in ovarian tumors is resistant to caspase-1 and -4 processing. *Oncogene*. 2004;23:7552–7560. doi: [10.1038/sj.onc.1208036](https://doi.org/10.1038/sj.onc.1208036)

31. Shi J, Zhao Y, Wang K, Shi X, Wang Y, Huang H, Zhuang Y, Cai T, Wang F, Shao F. Cleavage of GSDMD by inflammatory caspases determines pyroptotic cell death. *Nature*. 2015;526:660–665. doi: [10.1038/nature15514](https://doi.org/10.1038/nature15514)
32. Greenhough LA, Liang C-C, Belan O, Kunzelmann S, Maslen S, Rodrigo-Brenni MC, Anand R, Skehel M, Boulton SJ, West SC. Structure and function of the RAD51B-RAD51C-RAD51D-XRCC2 tumour suppressor. *Nature*. 2023;619:650–657. doi: [10.1038/s41586-023-06179-1](https://doi.org/10.1038/s41586-023-06179-1)
33. Gao S, Li G, Shao Y, Wei Z, Huang S, Qi F, Jiao Y, Li Y, Zhang C, Du J. FABP5 deficiency impairs mitochondrial function and aggravates pathological cardiac remodeling and dysfunction. *Cardiovasc Toxicol*. 2021;21:619–629. doi: [10.1007/s12012-021-09653-2](https://doi.org/10.1007/s12012-021-09653-2)
34. Iso T, Maeda K, Hanaoka H, Suga T, Goto K, Syamsunarno MRAA, Hishiki T, Nagahata Y, Matsui H, Arai M, et al. Capillary endothelial fatty acid binding proteins 4 and 5 play a critical role in fatty acid uptake in heart and skeletal muscle. *Arterioscler Thromb Vasc Biol*. 2013;33:2549–2557. doi: [10.1161/ATVBAHA.113.301588](https://doi.org/10.1161/ATVBAHA.113.301588)
35. D'Angelo A, Castillero E, Levy R, Ferrari G. Abstract 15006: serotonin transporter (SERT) knockout leads to increased myocardial and mitral valvular fibrosis in a murine model. *Circulation*. 2020;142:A15006. doi: [10.1161/circ.142.suppl_3.15006](https://doi.org/10.1161/circ.142.suppl_3.15006)
36. Ueland T, Nymo SH, Latini R, McMurray JJV, Kjekshus J, Yndestad A, Fucili A, Grosu A, Masson S, Maggioni AP, et al. CCL21 is associated with fatal outcomes in chronic heart failure: data from CORONA and GISSI-HF trials. *Eur J Heart Fail*. 2013;15:747–755. doi: [10.1093/eurjhf/hft031](https://doi.org/10.1093/eurjhf/hft031)
37. Troidl K, Rüdiger I, Cai W-J, Mücke Y, Grosseckler L, Piotrowska I, Apfelbeck H, Schierling W, Volger OL, Horrevoets AJ, et al. Actin-binding rho activating protein (Abra) is essential for fluid shear stress-induced arteriogenesis. *Arterioscler Thromb Vasc Biol*. 2009;29:2093–2101. doi: [10.1161/ATVBAHA.109.195305](https://doi.org/10.1161/ATVBAHA.109.195305)
38. Ahn J, Wu H, Lee K. Integrative analysis revealing human heart-specific genes and consolidating heart-related phenotypes. *Front Genet*. 2020;11:777. doi: [10.3389/fgene.2020.00777](https://doi.org/10.3389/fgene.2020.00777)
39. Kauffenstein G, Tamarelle S, Prunier F, Roy C, Ayer A, Toutain B, Billaud M, Isakson BE, Grimaud L, Loufrani L, et al. Central role of P2Y6 UDP receptor in arteriolar myogenic tone. *Arterioscler Thromb Vasc Biol*. 2016;36:1598–1606. doi: [10.1161/ATVBAHA.116.307739](https://doi.org/10.1161/ATVBAHA.116.307739)
40. Liu H, Liu P, Shi X, Yin D, Zhao J. NR4A2 protects cardiomyocytes against myocardial infarction injury by promoting autophagy. *Cell Death Discov*. 2018;4:27. doi: [10.1038/s41420-017-0011-8](https://doi.org/10.1038/s41420-017-0011-8)
41. Frangogiannis NG. The extracellular matrix in myocardial injury, repair, and remodeling. *J Clin Invest*. 2017;127:1600–1612. doi: [10.1172/JCI87491](https://doi.org/10.1172/JCI87491)
42. Pell VR, Chouchani ET, Murphy MP, Brookes PS, Krieg T. Moving forwards by blocking back-flow: the Yin and Yang of MI therapy. *Circ Res*. 2016;118:898–906. doi: [10.1161/CIRCRESAHA.115.306569](https://doi.org/10.1161/CIRCRESAHA.115.306569)
43. Li Y-F, Wei T-W, Fan Y, Shan T-K, Sun J-T, Chen B-R, Wang Z-M, Gu L-F, Yang T-T, Liu L, et al. Serine/threonine-protein kinase 3 facilitates myocardial repair after cardiac injury possibly through the glycogen synthase kinase-3 β /catenin pathway. *J Am Heart Assoc*. 2021;10:e022802. doi: [10.1161/JAHA.121.022802](https://doi.org/10.1161/JAHA.121.022802)
44. Ross RS, Borg TK. Integrins and the myocardium. *Circ Res*. 2001;88:1112–1119. doi: [10.1161/hh1101.091862](https://doi.org/10.1161/hh1101.091862)
45. Chopra A, Tabdanov E, Patel H, Janmey PA, Kresh JY. Cardiac myocyte remodeling mediated by N-cadherin-dependent mechanosensing. *Am J Physiol Heart Circ Physiol*. 2011;300:H1252–H1266. doi: [10.1152/ajpheart.00515.2010](https://doi.org/10.1152/ajpheart.00515.2010)
46. Tian R, Colucci WS, Arany Z, Bachschmid MM, Ballinger SW, Boudina S, Bruce JE, Busija DW, Dikalov S, Dorn GW, et al. Unlocking the secrets of mitochondria in the cardiovascular system: path to a cure in heart failure—a report from the 2018 National Heart, Lung, and Blood Institute workshop. *Circulation*. 2019;140:1205–1216. doi: [10.1161/CIRCULATIONAHA.119.040551](https://doi.org/10.1161/CIRCULATIONAHA.119.040551)